Simulation Research on the Depth Control of Remote Operated Vehicle Based on Single Neuron Pid

Zexin Jiang, Shaohan Chen

School of Automation, Beijing Information Science and Technology University, Beijing, China

Keywords: Remote operated vehicle, Depth control, Single neuron pid, Robustness, Simulink simulation

Abstract: For the depth control of ROV (remote operated vehicle), this paper established the function model of ROV motion process transfer according to the dynamics theory, and used PID control algorithm to control the depth. Considering the large disturbance in the process of depth keeping, the difficulty of getting accurate ROV model parameters, as well as the poor robustness and dynamic performance of traditional PID control, the neural PID controller is adopted. The simulation results show that the single neuron PID controller greatly improves the dynamic performance of the depth control. When the model parameters change slightly, it has better anti-interference performance and robustness.

1. Introduction

The ocean covers most of the earth, and contains rich resources such as flammable ice and submarine oil. The exploration of marine resources, the research of underwater species, as well as the salvage and other works all need the cooperation of ROV (remote operated vehicles). ROV with higher anti-interference ability also has higher working efficiency. Therefore, it is of great significance to study the control of ROV depth keeping [1].

The underwater environment is more complex; in the sea water, the motion of the remote operated vehicle is affected by the current at all times [2]. Meanwhile, the transfer function model of ROV often changes due to the change of mass or resistance area, so it is difficult to realize the precise control of ROV depth by using the traditional PID controller. References [3] and [4] propose to use the fuzzy control algorithm to carry out the adaptive control of ROV depth keeping. The experimental results show that the fuzzy control shows better control performance than the traditional control, but its regulation time is longer with poor rapidity. In this paper, combined with the supervised Hebb algorithm, a PID controller algorithm based on single neuron is established to improve the ROV depth keeping PID control, and a controller with shorter regulation time is designed. Simulation results show that the method has better dynamic performance, anti-interference and robustness.

2. Rov Control Object Model

2.1 Physical Model

The general design of ROV is shown in Figure 1. It is mainly composed of the frame structure, the cabin, the buoyancy block, the gravity block, the installation cushion block, the propeller and the mechanical arm. Table 1 shows the main materials, in which the mechanical arm is composed of ABS plastic and metal strut, and the circuit part in the cabin is replaced by metal block of the same quality.

  DOI: 10.25236/iwmecs.2020.061

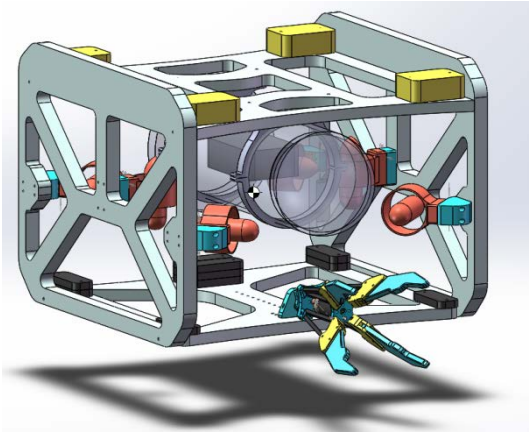

Fig.1 Rov Mechanical Model.

Table 1 Rov Materials.

name	material	Density (kg/m^3)
frame structure	PP polypropylene	933
cabin	acrylic	1190
buoyancy block	foam	16.0185
gravity block	Iron block	7300
installation cushion	ABS plastic	1020

The ROV designed is 0.46m in length, 0.46m in width, 0.35m in height and 13.089kg in mass. The center of gravity is 15.7cm from the bottom. ROV uses symmetrical design and counterweight to make the center of gravity in the horizontal plane.

The gravity material is concentrated at the bottom, and the buoyancy material is concentrated at the top, so that the center of gravity and the center of buoyancy of ROV are in the same straight line of the vertical plane, which can increase the stability of ROV. ROV is equipped with 6 thrusters, 4 in horizontal direction and 2 in vertical direction. The vertical thrust point is close to the horizontal plane where the center of gravity is located, and the horizontal thruster is 45 degrees inclination, in order to realize vector yawing when the thruster applies forces with different magnitudes and directions.

2.2 Mathematical Model

ROV will be subjected to gravity G and buoyancy F_f in water. The resistance of water is F_w. The effect of four thrust forces on the propeller is F_t. The dynamic equation between the combined external force F and the acceleration a is established according to Newton's Second Law.

$$\mathrm{F} = \mathrm{G} + F_f + F_w + F_T = \mathrm{ma} \tag{1}$$

$$F_w = \frac{C_k \rho v^2 A}{2} \tag{2}$$

In formula (2), C_k is the resistance coefficient, ρ is the density of water, v is the velocity of ROV moving in the vertical direction, and A is the area projected in its moving direction [5].

2.3 Establish the Transfer Function Model of the Control Object

This study only focuses on the vertical motion of ROV, so it is assumed that there is no dynamic force in the horizontal direction of the model and the resistance to water can be offset by the symmetry design of the model. In order to facilitate the establishment of the control model, it is necessary to simplify the mathematical model.

The machine should remain in suspension when there is no power, so it is assumed that the gravity G and buoyancy F_f of the machine are balanced in the water. The depth keeping process is a small range of low-speed fine adjustment process. After the process is linearized, the resistance

error of ROV at low speed of 0.1m/s is within 0.2N from the actual situation. It can be approximately considered that the linearized model is close to the actual situation at low speed.

$$F = C_k C_f \rho A v \tag{3}$$

Set C_f as the linearized scale factor. Let $\dot{h} = v$, $\ddot{h} = a$ [6], and bring them into equation (4) to get ROV, that is, the transfer function $G_h(s)$ between ROV depth and vertical thruster thrust:

$$G_h(s) = \frac{H(s)}{F_T(s)} = \frac{1}{ms^2 + C_k C_f \rho A s} \tag{4}$$

Wherein, water resistance area A = 0.0935m^2, C_k=1.2, C_f = 0.05, bring in relevant amount we can get:

$$G_h(s) = \frac{1}{13.089s^2 + 4.2063s} \tag{5}$$

In order to establish the model conveniently, the dimensionless gain between the input altitude error, the electric adjustment and the thruster thrust is taken as K_h=100 in this paper.

3. Design of Single Neuron Pid Controller for Depth Keeping Motion

3.1 Structure of the Single Neuron Pid Controller

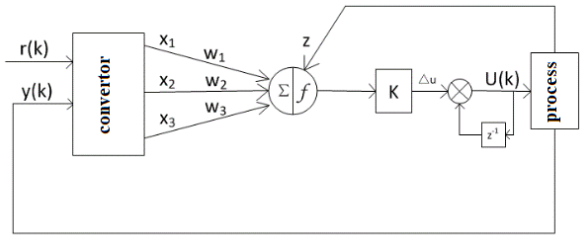

Fig.2 Structure of Single Neuron Pid Controller.

The structure of single neuron PID controller is shown in Figure 2 [7]. Among them, r (k) and y (k) are the input of the controller and the output of the system respectively; x_1, x_2 and x_3 are the input of the neuron and the state of the converter. w_1, w_2 and w_3 are the weights of x_1, x_2 and x_3 respectively. Z is the output of the system at the current time; K is the proportional coefficient of the neuron; △u and u (k) are the output variation and output of the controller respectively.

3.2 Algorithm of the Single Neuron Pid Controller

The single neuron PID controller adopts the improved supervised Hebb learning algorithm, which is shown as follows.

$$u(k) = u(k-1) + K\sum_{i=1}^{n} w_i'(k)x_i(k) \tag{6}$$

$$w_i'(k) = \frac{w_i(k)}{\sum_{i=1}^{n}|w_i(k)|} \tag{7}$$

$$w_i(k) = w_i(k-1) + \eta_i z(k)u(k)x_i(k) \tag{8}$$

In the equations, η is the learning rate; z (k) is the performance index or progressive signal; $w_i'(k)$ to w_i (k) is standardized [8]. In the single neuron PID controller, w_1, w_2 and w_3 represent the parameter proportion P, integral I and differential D in the PID controller. Therefore, $x_i(k)$ is defined as follows:

$$x_1 = \mathrm{e(k)} \tag{9}$$

$$x_2(\mathrm{k}) = \mathrm{e(k)} - \mathrm{e(k-1)} \tag{10}$$

$$\begin{aligned} x_3(k) &= \Delta e(k) - \Delta e(k-1) \\ &= e(k) - 2e(k-1) + e(k-2) \end{aligned} \tag{11}$$

Thus, the weight learning algorithm of single neuron PID controller can be obtained

$$w_1(k) = w_1(k-1) + \eta_I z(k) u(k) x_1(k) \tag{12}$$

$$w_2(k) = w_2(k-1) + \eta_P z(k) u(k) x_2(k) \tag{13}$$

$$w_3(k) = w_3(k-1) + \eta_D z(k) u(k) x_3(k) \tag{14}$$

For the three weights of proportional P, integral I and differential D, the controller adopts three different learning rates η_P, η_I and η_D, in order to adjust and control the learning rate of different parameters.

In a large number of practical applications, the modification of PID parameters is mainly related to $e(k)$ and $\Delta e(k)$, so we can optimize the weight updating part of the single neuron PID control algorithm derived in theory. The specific method is to replace $\mathrm{z}(k)$ with $e(k)$ and replace $\mathrm{x}_i(k)$ with $e(k) + \Delta e(k)$ [9]. The improved single neuron PID control algorithm is summarized as follows.

$$u(k) = u(k-1) + K \sum_{i=1}^{3} w_i'(k) x_i(k) \tag{15}$$

$$w_i'(k) = \frac{w_i(k)}{\sum_{i=1}^{3} \left| w_i(k) \right|} \tag{16}$$

$$\begin{aligned} &w_1(k) = w_1(k-1) + \\ &\eta_I e(k) u(k) (2e(k) - e(k-1)) \end{aligned} \tag{17}$$

$$\begin{aligned} &w_2(k) = w_2(k-1) + \\ &\eta_P e(k) u(k) (2e(k) - e(k-1)) \end{aligned} \tag{18}$$

$$\begin{aligned} &w_3(k) = w_3(k-1) + \\ &\eta_D e(k) u(k) (2e(k) - e(k-1)) \end{aligned} \tag{19}$$

4. Simulation Results and Analysis

The structure of single neuron PID controller is relatively complex. The existing Simulink module cannot achieve this function, so it needs to use the custom module to complete the simulation. The single neuron PID controller built in the custom module is shown in Figure 3.

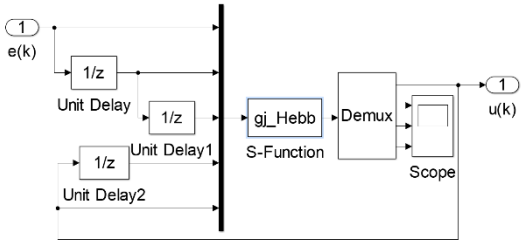

Fig.3 Single Neuron Pid Controller.

Among them, gj_Hebb module is a supervised Hebb learning algorithm written by S-function module, through which PID parameters can be adjusted automatically. *e(k)* and *u(k)* are the input and output of single neuron PID controller respectively. The overall simulation framework of ROV depth control system is shown in Figure 4.

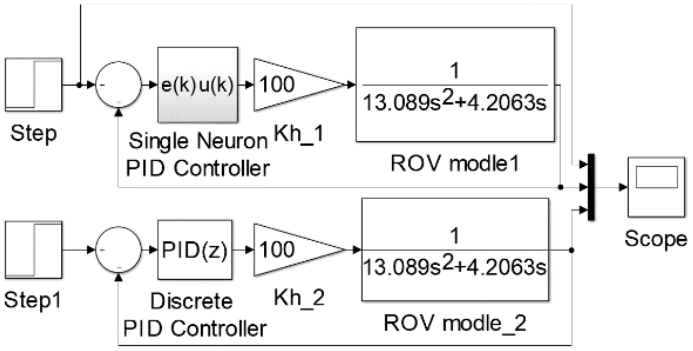

Fig.4 Overall Simulation Framework.

In the process of simulation, the learning rates η_P, η_I , η_D and proportional coefficient K are adjusted repeatedly to find the most appropriate parameters, so that the single neuron PID controller can adjust PID parameters to a more appropriate size in a very short time.

After several adjustments of parameters, we finally determined η_P =0.8, η_I =0.001, η_D =1000, and K=2000. The single neuron PID controller is compared with the traditional PID controller which has completed the parameter tuning (represented by SPID and TPID respectively). The response curves of the two controllers are shown in Figure 5; overshoot σ and adjustment time t_s are shown in Table 2.

Table 2 Dynamic Comparison.

	σ/%	ts/s
SPID	4.8	2.167
TPID	14	19.065

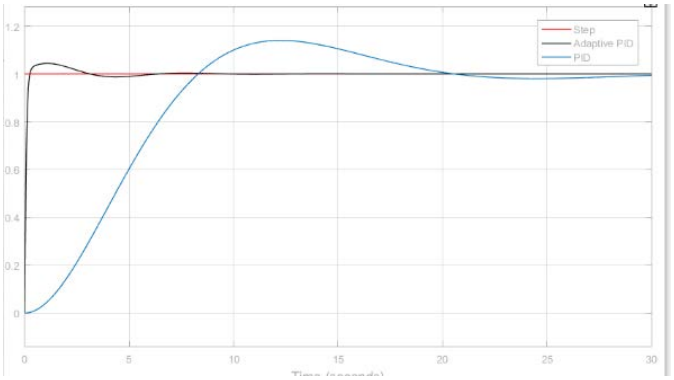

Fig.5 Comparison of Simulation Results.

Compared with the traditional PID controller, the dynamic performance of the single neuron PID controller is obviously improved. The adjustment time and overshoot are greatly reduced, so that ROV can track the given signal more smoothly and quickly when it is subject to external interference.

In practical application, the parameters of transfer function of the ROV model often change to some extent. The transfer function of ROV is equation (5). The quadratic coefficient of the denominator of the transfer function T1 is reduced by 0.5 times; the coefficient of the primary term T2 is reduced by 0.5 times; the size of T2 is increased by 0.5 times. The simulation results are compared with those of the original model.

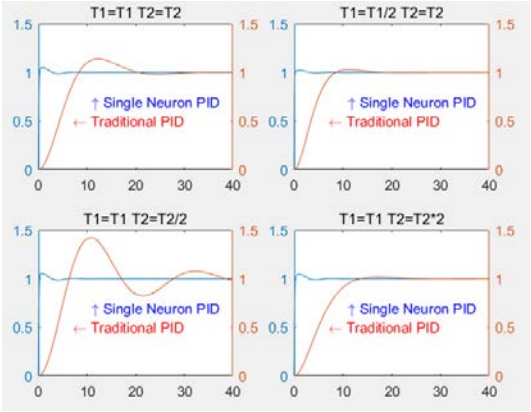

Fig.6 Simulation Results When Model Parameters Change.

Table 3 shows that when ROV model parameters change by 50%, σ in SPID response increases by 0.5%. The maximum increase of TPID was 28.1%; the maximum increase of t_s in SPID response was 0.13s, and the maximum increase of TPID was 27.26s. In comparison, when the system parameters change, the single-neuron PID controller has better dynamic performance, anti-interference and robustness.

Table 3 Parametric Response.

	σ/%	t_s/s
SPID(T1=T1/2)	2.1	1.352
TPID(T1=T1/2)	2.8	13.346
SPID(T2=T2/2)	5.3	2.073
TPID(T2=T2/2)	42.1	46.325
SPID(T2=T2*2)	4.4	2.297
TPID(T2=T2*2)	1.6	12.297

5. Conclusion

In this paper, the single neuron PID control is applied to ROV control model. The experimental results show that the dynamic performance of the controller is better than that of the traditional PID controller, and the control effect is better when model parameters of the control object change slightly. When the parameters of ROV model change in a certain range under the influence of external forces or its own mechanical structure, the single neuron PID controller enables ROV to realize depth control quickly and accurately. This method has good anti-interference and robustness, and has important reference value for the ROV depth control.

References

[1] Liu, X., Wei, Y.H., Gao, Y.B. Overview of ROV Motion Control Technology. Journal of Chongqing University of Technology (Natural Science), vol. 28, no. 07, pp. 80-85, 2014.

[2] Li, B., Mo, J. Assessment of the Influence of Current on the Navigation Safety of Remote Operated Vehicles. Ship Science and Technology, vol. 34, no. 08, pp. 31-34, 2012.

[3] Qi, S.B., Yin, B.A., Su, Z.K. Simulation of Small ROV Depth Keeping Motion Control Based on Fuzzy PID. Modern Electronics Technique, vol. 43, no. 02, pp. 20-23, 2020.

[4] Silvia, M. Giuseppe, C. Remotely Operated Vehicle Depth Control. Control Engineering Practice, vol. 11, no. 4, pp. 453-459, 2003.

[5] Chen, Y., Zhang, Y., Zhao, R.Y., et. al. Design of ROV Heading Control System Based on Fuzzy PD-PI Method. Computer Applications and Software, vol. 36, no. 12, pp. 106-110, 2019.

[6] Liu, M.M., Ying, Z.Q, Liang, B.Y., et. al. Experimental Study on the Motion Characteristics of Rammer in Water. Port and Waterway Engineering, no. 03, pp. 173-177, 2017.

[7] Shu, D.Q., Li, C.T., Yin, Y.X. Single Neuron Adaptive PID Controller and its Application in Electric Heating Furnace. Electric Drive, vol. 25, no. 1, pp. 29-32, 1995.

[8] Eissa, M.A. Novel Fuzzy-Based Self-Adaptive Single Neuron PID Load Frequency Controller for Power System. Power Electronics and Drives, vol. 4, no. 1, pp. 141-150, 2019.

[9] Liu, J.K. Matlab Simulation of Advanced PID Control, Third Edition, Beijing: Publishing House of Electronics Industry, 2011, pp.237-256.